



Interfacial properties of nanosilica-treated structural polymer fibres in cement matrix composites



Su-Jin Lee^a, Shiho Kawashima^a, Ki-Joong Kim^b, Sang-Kyun Woo^c, Jong-Pil Won^{d,*}

^a Department of Civil Engineering and Engineering Mechanics, Columbia University, New York 10027, USA

^b Construction Engineering & IT Service (CENITS) Corporation Inc., Seoul 08501, Republic of Korea

^c Korea Electric Power Corporation Research Institute, Structural & Seismic Tech. Group, Daejeon 34056, Republic of Korea

^d Department of Civil & Environmental System Engineering, Konkuk University, Seoul 05029, Republic of Korea

ARTICLE INFO

Keywords:

Bond strength
Fiber reinforced
Nano-silica
Self-healing
Sol-gel
Surface treatment

ABSTRACT

In this study, silica nanoparticles formed on the surface of structural polymer fibres improved bonding with the cement matrix and provided a self-healing function when cracking occurred in the composite. Silica nanoparticles were formed via a sol-gel process on fibre surfaces; these treated fibres were dried at room temperature and 50 °C. Observation of the fibre surfaces by digital microscopy confirmed the formation of silica nanoparticles on the fibre surfaces. The amount of silica nanoparticles produced on the surface was quantitatively determined by the change in mass before and after the surface treatment. Measurements of the water absorption and amount of soluble matter lost confirmed that the surface of the hydrophobic structural polymer fibres had been modified. The interaction between the nanosilica-treated structural polymer fibres and cement matrices was evaluated using a single-fibre bond test. This test showed that the nanosilica-treated fibres had a maximum pull-out strength and interfacial toughness that were 104.1–113.4% and up to 120% higher, respectively, than those of the untreated fibres.

1. Introduction

Well-designed cement composites achieve high strength through a tight microstructure. This prevents defects such as cracks from occurring, as well as propagation of such cracks, in the composite. However, cementitious materials already have microcracks at the interface before any external load is even applied because of the shrinkage deformation that occurs during drying [1,2].

However, cracks in reinforced concrete (RC) do not imply structural damage, failure or safety problems. Cracks that are excessively wide may lead to corrosion of reinforcing bars; such corrosion is a major cause of premature failure of concrete structures [2–6]. The presence of cracks can also reduce the durability of RC structures.

Concrete structures are generally defined in terms of the performance and life expectancy (durability) that is identified at the time of the design; longevity is achieved through maintenance programs. Recently, new approaches have been developed to improve the durability of structures using materials that are adaptable or self-healing over time [2,7–10].

There are two types of self-healing materials, namely, autogenic and autonomic. Cementitious materials have an innate autogenic ability to self-heal. Unhydrated cement particles remaining in the cement matrix

of cementitious composites can hydrate if they are exposed to water. Autonomic cement composites contain foreign materials that enable a response to cracking [2,10,11]. Notably, materials such as fly ash, silica fume, and silica nanoparticles, which can generate reaction products through a pozzolanic reaction similar to the hydration reaction of cement particles, are incorporated into cement matrices. This is different from the approach of maximising the amount of reaction products in cement composites via autogenic self-healing [9,10,12–14].

Crack width plays a very important role in the self-healing process. Typically, narrow cracks have a greater chance of being filled than wide cracks. Many studies have suggested that the crack width should be 200 µm or less to promote self-healing, and some have indicated that the optimal crack width ranges from 20 to 60 µm [15]. The most common way to control critical crack widths for self-healing is to use reinforcing fibres, which constitutes an autonomic self-healing approach [2–8,15].

Summarising, cement composites have autogenic self-healing abilities and self-healing can be induced through the incorporation of foreign materials. The narrower the crack, the more likely it is to heal, and with greater efficiency. Accordingly, in this study, we explored the deposition of reactive nanomaterials on a fibre surface to potentially control the crack width and thereby improve self-healing of cement

* Corresponding author.

E-mail address: jpwon@konkuk.ac.kr (J.-P. Won).



Fig. 1. Structural polymer fibres used in the study.

composites. Specifically, silica nanoparticles were deposited on the surface of structural polymer fibres using a sol-gel method; their presence was confirmed by microscopy and a water absorption test. Additionally, the bond between the nanosilica-treated structural polymer fibres and the cement matrix was characterised by fibre pull-out behaviour among other properties.

2. Materials and mix proportions

2.1. Structural polymeric fibre

The structural polymer fibre used in this study was of the macro type (MasterFibre 246; BASF, Germany) with a diameter of 0.75 mm and a length of 40 mm. The fibre shapes are shown in Fig. 1 and their properties in Table 1.

2.2. Surface treatment method

A sol-gel process was used to synthesise silica nanoparticles on the surface of the structural polymer fibres [16–22]. The sol-gel reaction consists of two steps, i.e. hydrolysis of silicon alkoxide followed by a condensation reaction. The shape and size of the formed silica nanoparticles were affected by the precursor, reactants, solvent, pH, synthesis temperature and other reaction conditions [16–20]. In this study, we used ethanol as the solvent for the sol-gel reaction, ammonia solution (28 wt% NH₄OH; Sigma–Aldrich, USA) for the hydrolysis reaction and tetraethyl orthosilicate (TEOS; Sigma–Aldrich) as the precursor of the silica nanoparticles. High-purity reactants were used in all cases. The reaction temperature was controlled at 50 °C.

2.2.1. Pre-treatment

The same temperature condition (50 °C) was used throughout the entire sol-gel process (hydrolysis, condensation reaction and drying after the reaction). All of the materials used in the sol-gel reaction were conditioned in a 50 °C oven until immediately before use. The structural polymer fibres used in this study were polypropylene fibres, which do not absorb moisture from the air (Table 1). Nevertheless, the fibres

were conditioned at 50 °C to have the same thermal history as the other materials.

2.2.2. Hydrolysis and condensation

An alkaline reaction environment was established using 28% ammonia solution and TEOS was used as the precursor of the silica nanoparticles. The solutions used in the hydrolysis and condensation phases of the sol-gel reaction were as follows. Structural polymer fibres (2 g) were placed in a flask containing ethanol (200 g), ammonia solution (30 g) and distilled water (20 g). The suspension was maintained at 50 °C for 10 min. Then, TEOS (40 g) was added and the mixture was stirred for 60 min using a magnetic stirrer. The structural fibres were removed by filtration after 1 h, washed with distilled water and then dried in an oven at room temperature or at 50 °C for 48 h. Herein, the untreated structural polymer fibres are designated as UMP, the fibres dried at room temperature after the sol-gel process as RMP and the fibres oven-dried at 50 °C as OMP.

2.3. Cement matrix

The bond properties of the nanosilica-treated structural polymer fibres were examined using cement paste as the matrix to eliminate the effect of aggregate. The cement was Type I Portland cement with a specific gravity of 3.15. The paste was formed at a water–cement ratio of 0.4.

3. Experimental

3.1. Silica nanoparticles on the fibre surface

Microscopic observation of the surfaces and mass changes confirmed the formation of nanosilica particles on the surface of the structural polymer fibres via the sol-gel process. The water absorption test carried out according to the ASTM D570 standard confirmed that the hydrophobicity of the structural polymer fibres had been modified by the formed silica nanoparticles. Repeated water absorption tests established the loss of soluble matter from the treated fibres [23].

Table 1
Fibre properties.

Type of polymer	Diameter (mm)	Length (mm)	Density (g/cm ³)	Melting point (°C)	Tensile strength (MPa)	Water absorption (%)	Chemical resistance
Polypropylene	0.75	40	0.9	160 ± 5	425 ± 25	0	High

The water absorption test is greatly affected by temperature. The fibres used in this test were oven-dried at 50 ± 3 °C for 24 h, cooled to room temperature in a desiccator and then weighed (conditioned weight) to a precision of 0.001 g. Then, they were completely immersed in distilled water at 23 ± 1 °C for 24 ± 0.5 h. The mass of fibres was then removed from the water bath, excess water was removed and the mass (wet weight) was measured. The water absorption was calculated using Eq. (1):

$$\text{Water absorption}(\%) = \frac{\text{wet weight} - \text{conditioned weight}}{\text{conditioned weight}} \times 100 \quad (1)$$

The water solubility of particles on the surface of the structural polymer fibres was determined as follows. The fibres immersed in distilled water for the water absorption test were dried again in the oven at 50 ± 3 °C for 24 h. After cooling to room temperature in a desiccator, the mass was measured (reconditioned weight) to a precision of 0.001 g. The soluble matter lost was calculated using Eq. (2):

$$\text{Soluble matter lost}(\%) = \frac{\text{conditioned weight} - \text{reconditioned weight}}{\text{conditioned weight}} \times 100 \quad (2)$$

3.2. Bond properties of the nanosilica-treated fibres

The bond properties of the nanosilica-treated structural polymer fibres were evaluated according to the JCI-SF8 standard. A cement paste made at a water-cement ratio of 0.4 was used as the cement matrix. This eliminated any effect of aggregate at the fibre-cement matrix interface. Fig. 2 shows the test specimen and the set-up used in the bond properties test.

A single fibre was fixed to the centre of a two-part dog-bone-shaped specimen using a partitioning board (Fig. 2(a)), and then cement paste was placed in each of the divided parts. Initial curing was carried out in a constant temperature and humidity room at 23 ± 2 °C and $50 \pm 5\%$ relative humidity for 24 h, followed by curing for 28 days in a water tank at 23 ± 2 °C. Samples were only half-immersed, rather than fully immersed, to avoid disappearance of the nanosilica formed on the fibre surfaces; the portion exposed to the air was covered with a wet cloth to maintain the same condition as underwater curing. After 28 days of curing, specimens were placed as shown in Fig. 2(b) and then loaded under displacement control at 0.5 mm/min using a universal testing machine equipped with a 5-kN load cell (Model 3369; Instron®, USA).

4. Results and discussion

4.1. Observations of the fibre surface

Fig. 3 shows digital microscopy images acquired at $100 \times$ magnification of the surfaces of individual structural polymer fibres before and after the sol-gel reaction. The transparency of the pre-reaction structural polymer fibre is notable (Fig. 3(a)). Fig. 3(b) shows the surface of an RMP fibre after the sol-gel reaction, while Fig. 2(c) shows the surface of an OMP fibre. Silica nanoparticles (encircled) are clearly seen on the fibre surfaces for both types of treated fibres, although the nanoparticles are not uniformly distributed; these treated fibres were translucent. The treated fibres oven-dried at 50 °C had more uniformly dispersed particles.

Nanoparticles tend to agglomerate when dispersed in liquids. Therefore, the reaction solution cooled to room temperature after the sol-gel reaction was filtered and then dried for 48 h. The solution evaporated more quickly during oven drying, which resulted in agglomeration of the silica nanoparticles. Drying of the solution at room temperature over 48 h likely did not completely remove water inside the hydrophilic particles. Therefore, we assumed that they contained some residual moisture even after drying, and that the silica nanoparticles were also aggregated.

4.2. Changes in mass

Masses were recorded before and after the sol-gel reaction to confirm the formation of nanosilica on the surface of the structural polymer fibres. All fibres were stored in a desiccator filled with absorbent (silica gel beads) at room temperature to prevent any possible mass change due to moisture in the air, and were removed just before the mass measurement. Table 2 summarises the mass changes before and after the sol-gel reaction.

The mass changes revealed that the nanosilica-treated fibres increased in mass by 14.2% (RMP) and 9.59% (OMP). This compares with no mass change for the UMP fibres, regardless of the drying environment. The increased mass after the sol-gel reaction, which was attributed to the silica nanoparticles, was 12.5% and 8.75% for the RMP and OMP fibres, respectively. The mass change for the OMP fibres was smaller than that for the RMP ones. This reflected the drying environment, rather than any change in the absolute amount of nanosilica particles.

4.3. Water absorption and soluble matter lost tests

The purpose of this study was to render the intrinsic hydrophobic properties of the polypropylene fibres more hydrophilic by generating

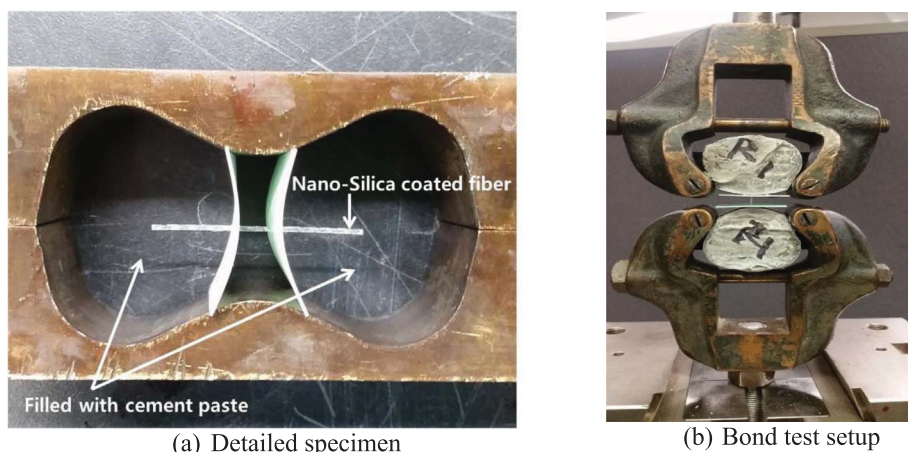


Fig. 2. Single-type bond test set-up.



(a) Untreated structural polymer fibre (UMP)



(b) Dried at room temperature after sol-gel treatment(RMP)



(c) Dried at 50°C after sol-gel treatment(OMP)

Fig. 3. Fibre surfaces before and after the sol-gel treatment.**Table 2**
Changes in mass of the structural synthetic fibres after the sol-gel treatment.

	UMP	RMP	OMP
Mass (g)	1.679	1.918	1.840
Increase in mass (g)	–	0.239	0.161
Increase in mass (%)	–	14.2	9.59
Nanosilica on the treated fibre (%)	–	12.5	8.75

Table 3
Water absorption and soluble matter of the nanosilica-treated fibres.

	UMP	RMP	OMP
Conditioned weight (g)	0.155	0.156	0.159
Wet weight (g)	0.155	0.158	0.162
Reconditioned weight (g)	0.155	0.156	0.159
Water absorption (%)	0.000	1.713	2.101
Soluble matter lost (%)	0.000	0.000	0.000

silica nanoparticles on the surface of the fibres via a sol-gel method. Water absorption was one indicator of improved hydrophilicity. Soluble matter loss, which was attributed to the loss of nanosilica from the fibre surfaces, was another indicator. Table 3 summarises the water absorption and soluble matter loss test results for the structural polymer fibres before and after the sol-gel process.

Water absorption testing revealed that the untreated (UMP) fibres

did not absorb water, while all of the fibres treated using the sol-gel method absorbed water regardless of the drying condition (Table 1). The water absorption was 1.713% for the RMP fibres and 2.101% for the OMP fibres. However, the mass change before and after the sol-gel process was smaller for the OMP fibres than for the RMP ones. This apparent discrepancy was attributed to the difference in moisture content of the silica nanoparticles, rather than to any difference in the absolute amount of nanosilica, as noted above. The silica nanoparticles on the OMP fibre surfaces absorbed relatively more water than the RMP fibres when in contact with water, because the nanosilica particles on the surface of OMP fibre surfaces were drier.

The loss of soluble matter of a sample was established by comparing the dried masses before and after 24 h of immersion. The base polypropylene fibres are insoluble in water. Fibre surfaces were observed before and after immersion to support the water absorption and soluble matter loss results (Fig. 4). Despite being immersed in distilled water for 24 h, both types of nanosilica-treated fibres (RMP, OMP) retained the generated silica nanoparticles on their surfaces.

4.4. Bond properties of the nanosilica-treated fibres in a cement matrix

The bond properties of the treated structural polymer fibres are illustrated in Fig. 5. The maximum pull-out resistance load, displacement and interfacial toughness for each fibre type are shown in Fig. 6 and are summarised in Table 4.

The solid curve in Fig. 5 represents the average value for each fibre type (UMP, RMP and OMP), but the maximum and minimum values

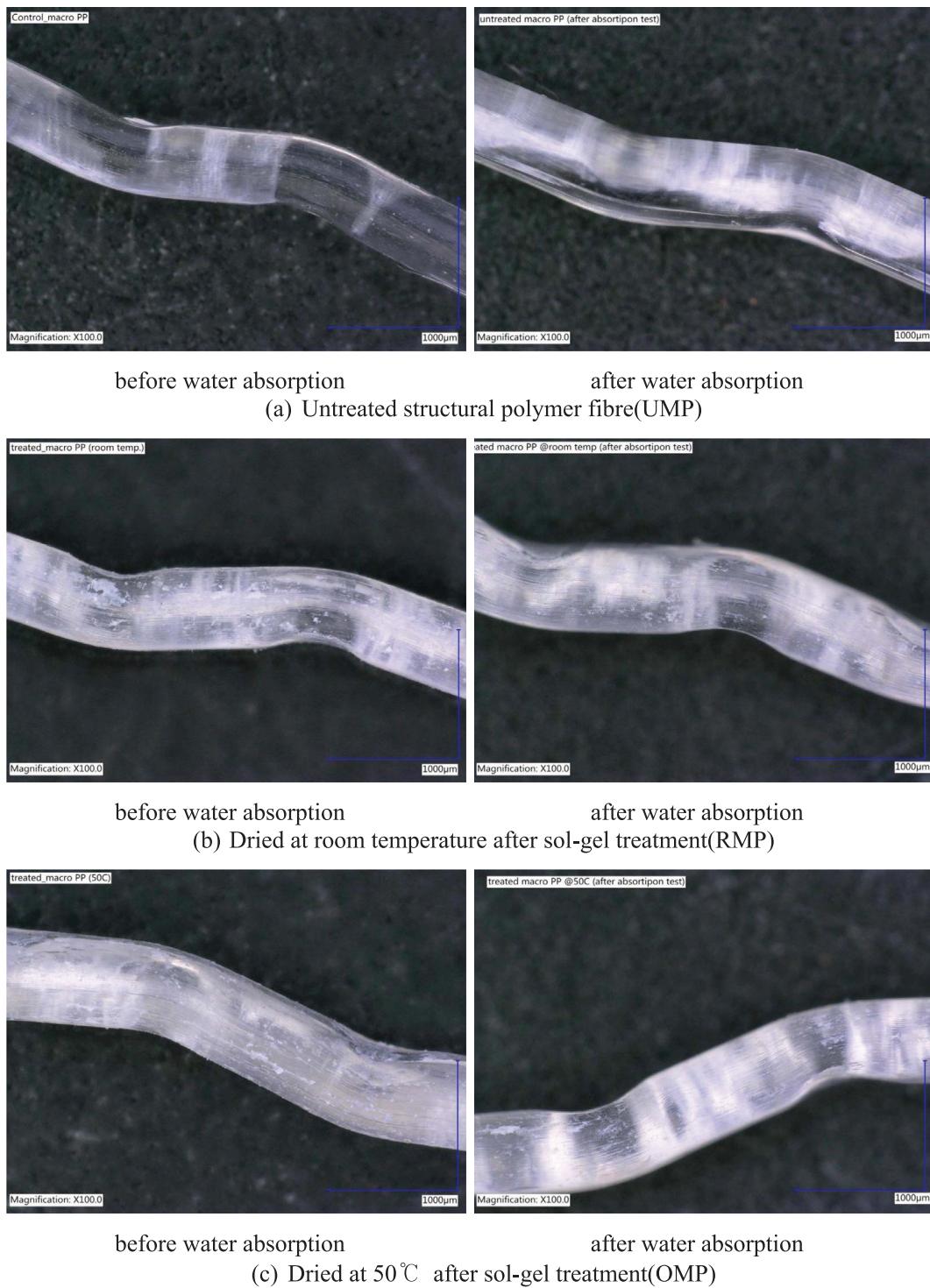


Fig. 4. Nanosilica-treated fibre surfaces before and after water absorption testing.

were excluded from the average calculation to aid comparisons. The bond properties of both nanosilica-treated fibres (RMP and OMP) were improved over those of the UMP fibres. Pull-out load–slip behaviour is shown in Fig. 5; a stronger bond between the cement matrix and fibres results in a higher pull-out resistance load (the maximum load). The nanosilica-treated structural polymer fibres of this study displayed higher maximum loads and pull-out displacement (slip) from the cement matrix (Fig. 5(b), (c), and Table 4).

The embedded length of a fibre in the cement matrix was 17 mm. The UMP fibres displayed a shorter pull-out displacement than the

embedded length of fibre. This meant that after the fibres were separated from the cement matrix, i.e. after the peak load, there was little pull-out resistance caused by friction with the cement matrix, which enabled facile pull-out. This behaviour was consistent with the poor bond properties of the hydrophobic polymer fibres. However, the nanosilica-treated structural polymer fibres (RMP and OMP) displayed pull-out displacements that were equal to the embedded length, and there was higher resistance to pull-out due to frictional forces between the fibres and the cement matrix with continued separation. Thus, the silica nanoparticles formed on the surface of the structural polymer

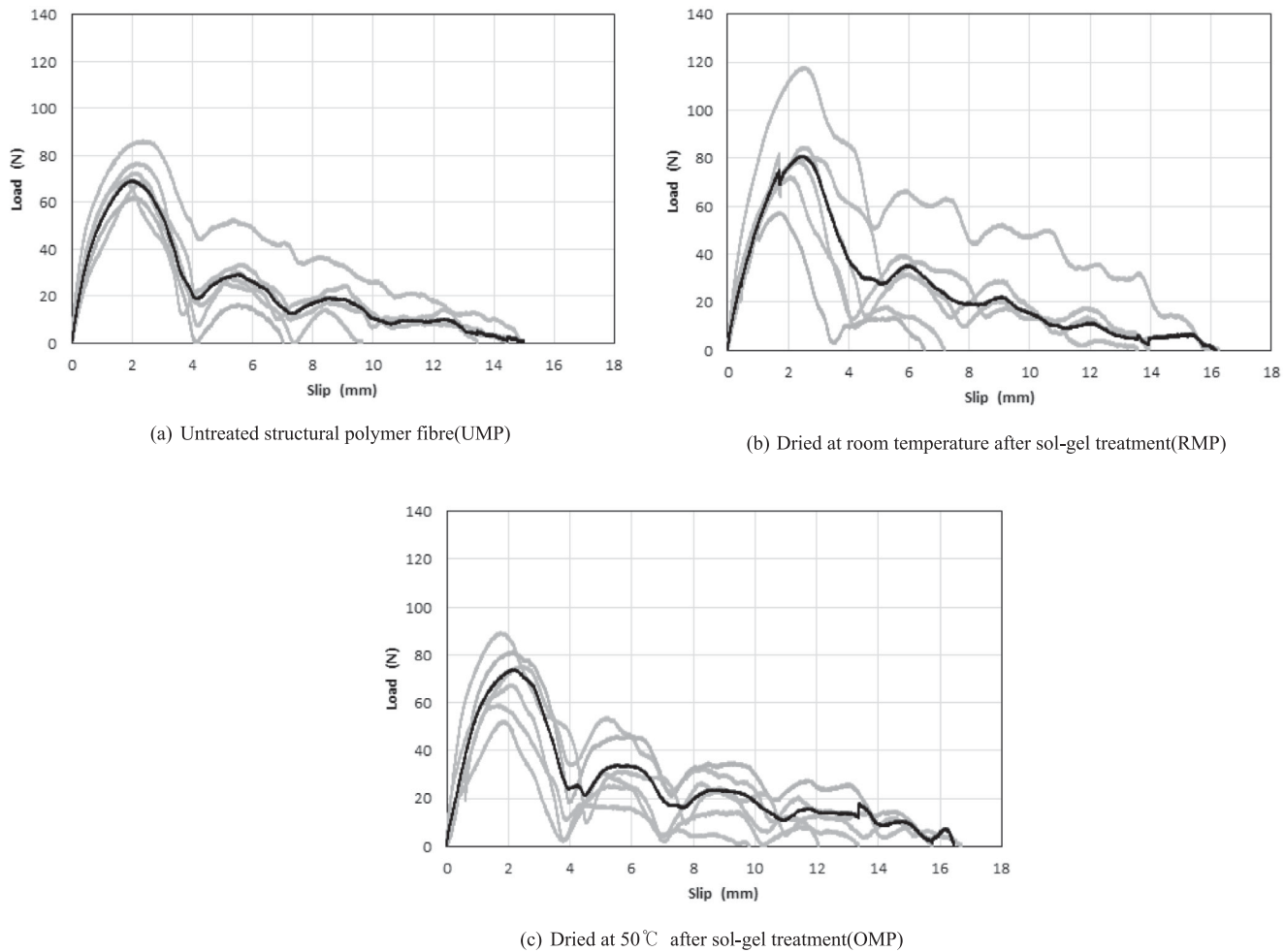


Fig. 5. Pull-out load-slip curves of nanosilica-treated fibres.

fibres modified the hydrophobic surface to a hydrophilic one and thereby improved bonding to the cement matrix. Relative to the UMP fibres, the maximum pull-out strength and maximum displacement were enhanced by 113.4% and 230.2%, respectively, for the RMP fibres and by 104.1% and 234.2%, respectively, for the OMP fibres (Fig. 6(a)).

The interfacial toughness noted in Table 4 is the resistant energy (N·mm) against pull-out or fracturing as the fibre is pulled out from the cement matrix to a specific displacement. The JCI-SF8 standard specifies that only the initial interfacial toughness (energy to 5 mm of pull-out displacement) is measured when the bond test is performed on a single fibre. However, 10 mm of pull-out displacement was used herein in consideration of the 17-mm embedded length of the fibres. The pull-out displacement was less than 10 mm for some untreated polymer fibres. In this case, the maximum pull-out displacement was calculated as the final interfacial toughness (energy to 10 mm). Relative to the UMP fibres, the initial and final interfacial toughnesses improved by 119.8% and 121.5%, respectively, for the RMP fibres. However, the OMP fibres had initial and final interfacial toughnesses of 97.0% and 95.0%, respectively, which was about 5% lower than for the UMP case. This can be related to the results discussed in Section 4.3. The OMP fibres were much drier compared to the RMP ones. It is believed that the cement matrix around an OMP fibre had reduced strength because the mixing water was more absorbed at the fibre–cement matrix interface before cementing. In other words, although the silica nanoparticles on the fibre surface provided some hydrophilicity, the strength of the cement matrix surrounding the fibre was nevertheless lower due to excessive absorption of chemically combined water at the fibre–cement matrix interface.

Fig. 6 shows images of single nanosilica-treated structural polymer fibres after pull-out from the cement matrix. Microscopic examination of the part of a fibre pulled out from the cement matrix provided information on the pull-out resistance of the fibre at the fibre–cement matrix interface. The overall appearance of the pulled-out area was best seen at low magnification (20 \times , left-hand images). Fig. 6(a) shows the pulled out portion of a UMP fibre; it was less damaged than the nanosilica-treated fibres (Fig. 6(b) for RMP, Fig. 6(c) for OMP). Notably, the ends of the fibres, where most damage occurred, were more frayed for the nanosilica-treated fibres. Overall, the RMP fibre was more damaged than the OMP one, which is consistent with the higher pull-out resistance of the room temperature-dried fibre.

High-magnification images (100 \times , right-hand side) show UMP fibres that were scratched and partly cracked during fibre pull-out, and no cement matrix or other product is evident. Friction marks, cement matrix particles in some cracks and reaction products from the nanosilica formation can be seen on the nanosilica-treated fibre surface (encircled areas).

5. Conclusions

Surface functionality was provided to synthetic polymer fibres by synthesising and depositing silica nanoparticles through a sol-gel process. The presence of these particles was confirmed qualitatively and quantitatively by microscopy, mass change and water absorption tests, before and after the sol-gel reaction. Additionally, the effect of the silica nanoparticles on the interface was revealed through the bond properties between the nanosilica-treated fibres and the cement matrix. The

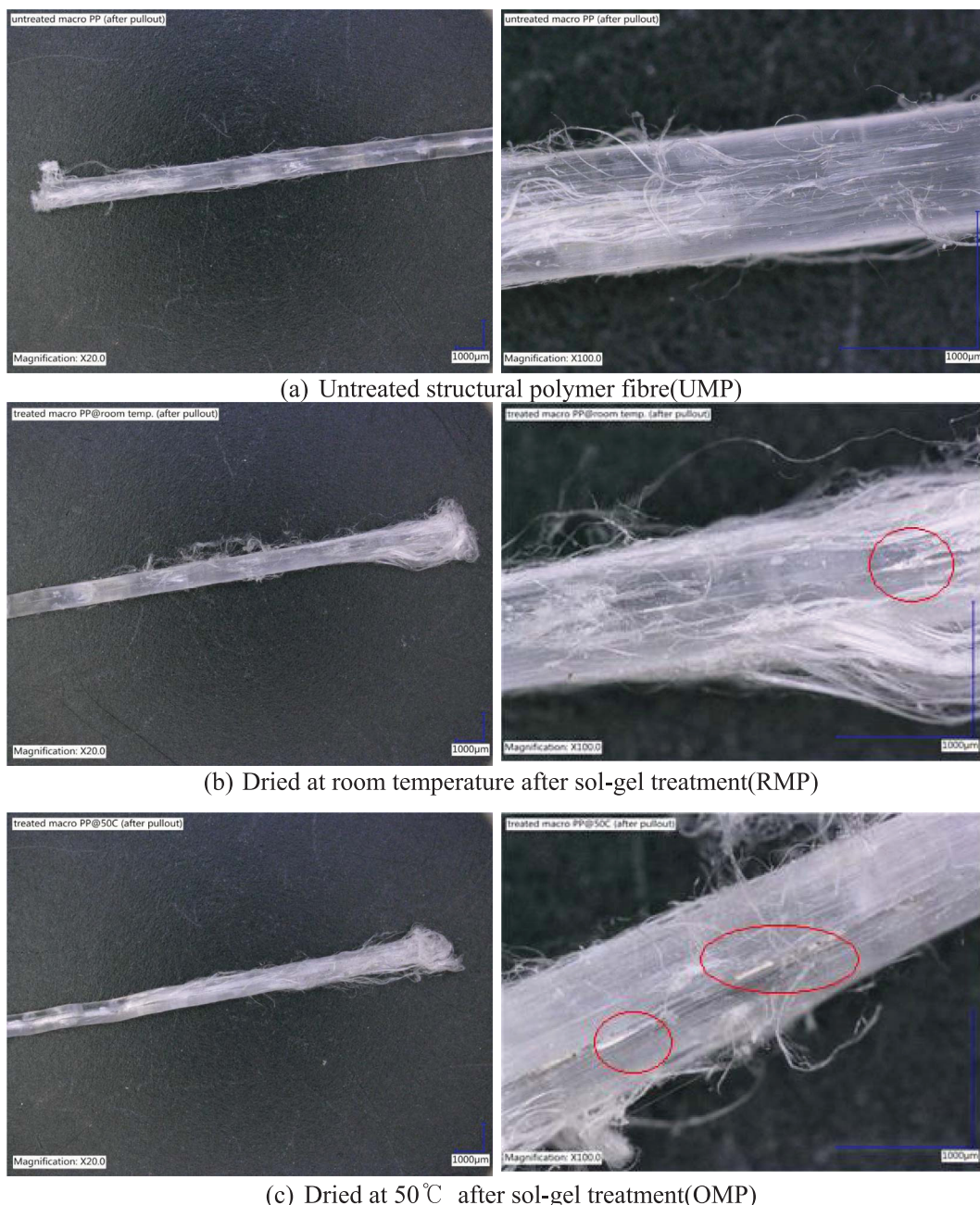


Fig. 6. Nanosilica-treated fibre surfaces after pulling out.

Table 4

Bond properties of the nanosilica-treated fibres.

	UMP	RMP	OMP	
Maximum load (N)	72.0	81.8	75.0	
Maximum slip (mm)	14.3	16.2	16.5	
Interfacial toughness (N-mm)	Energy to 5 mm	218.0	261.2	211.4
	Energy to 10 mm	315.2	382.9	299.6

results of this study are summarised as follows:

1. Hydrophilic functional particles were formed on the surface of a structural polymer fibre via a sol-gel process. Microscopy revealed the presence of silica nanoparticles on the surface of fibre, which were retained regardless of the drying condition. Notably, the treated fibres dried at room temperature had larger nanoparticles

than those on fibres dried at 50 °C. We also quantitatively established the amount of silica nanoparticles produced by measuring the mass change before and after the sol-gel process.

2. Water absorption tests on the fibres confirmed that the silica nanoparticles generated on the surface modified the fibre hydrophobicity, which is characteristic of polyolefin fibres. Additionally, the presence of water-soluble materials was confirmed, consistent with the silica nanoparticles. The UMP fibres did not absorb water, while the nanosilica-treated ones absorbed about 2% water. It was also established that the nanosilica particles deposited on the fibre surfaces were not lost when in contact with the mixing water of the cement.
3. Bond tests quantified the interaction between the surface-modified fibres and the cement matrix. The bond properties of the structural nanosilica-treated polymer fibres were better than those of the UMP fibres, regardless of the drying conditions after the sol-gel reaction.

The higher maximum pull-out resistance load indicated that the fibre–cement matrix bond was quite robust, and the mechanical properties of the interface were improved through the silica nanoparticles present on the surface of the fibres. Additionally, the treated fibres pulled out under a relatively higher pull-out load compared with UMP fibres. The pull-out displacement from the cement matrix was also improved because of the greater frictional resistance resulting from better interfacial properties.

4. Observations of the surfaces of nanosilica-treated structural fibres pulled out from the cement matrix provided evidence of frictional resistance against the pulling load. Compared with UMP fibres, the nanosilica-treated ones had larger frictional marks and some surface cracks. Additionally, particles of cement matrix and reaction products produced through the nanosilica synthesis were observed at damaged parts of the fibre surface and surroundings.

Acknowledgements

This research program was funded by Korea Electric Power Corporation Research Institute (KEPCO-RI) of Korea, and its kind support is gratefully acknowledged.

References

- [1] Metha P Kumar, Monteiro Paulo JM. Concrete-microstructure, properties, and materials (Third edition). McGraw-Hill; 2006. 49–67, 95–108.
- [2] Hager Martin D, Greil Peter, Leyens Christoph, van der Zwaag Sybrand, Schubert Ulrich S. Self-Healing Materials. *Adv Mater* 2010;22:5424–30.
- [3] Choi Heesup, Inoue Masumi, Kwon Sukmin, Choi Hyeyonggil, Lim Myungkwan. Effect crack control of concrete by self-healing of cementitious composites using synthetic fiber. *Materials* 2016;9(4):248–61.
- [4] Herbert Emily N, Li Victor C. Self-Healing of microcracks in engineered cementitious composites (ECC) under a natural environment. *Materials* 2013;6:2831–45.
- [5] Homma Daisuke, Mihashi Hirozo, Nishiwaki Tomoya. Self-healing capability of fibre reinforced cementitious composite. *J Adv Concr Technol* 2009;7(2):217–28.
- [6] Cuenca E, Ferrara L. Self-healing capacity of fiber-reinforced cementitious composites: State of the art and perspective. *KSCE J Civ Eng* 2017;21(7):2777–89.
- [7] Klaas van Breugel. Self-healing material concrete as solution for aging infrastructure. In: Proceeding of the 37th conference on our world in concrete & structure; 29–31 August 2012. Singapore.
- [8] Li Victor C, Yang En-Hua. Self healing in concrete materials. *Self Healing Materials: an alternative approach to 20 centuries of material*. Springer; 2007. 161–193.
- [9] Biricik Hasan, Sarier Nihal. Comparative study of the characteristics of nano-silica-, silica fume- and fly ash-incorporated cement mortar. *Mater Res* 2014;17(3):570–82.
- [10] de Rooij Mario, Van Tittelboom Kim, De Belie Nele, Schlangen Erick. Self-healing phenomena in cement-based materials. *State-of-the-Art Report of RILEM Technical Committee 221-SHC*. Springer; 2013. 1–17, 65–214.
- [11] Hearn Nataliya. Self-sealing, autogenous healing and continued hydration: What is the difference? *Mater Struct* 1998;31:563–7.
- [12] Lucas Sandra S. Development of self-healing cement pastes by long-term hydration. In: Proceeding of the 6th international conference on self-healing materials (ICSHM 2017); 25–28 June 2017. Germany.
- [13] Termkhajornkit Pipat, Nawa Toyoharu, Yamashiro Yoichi, Toshiki Saito. Self-healing ability of fly ash-cement systems. *Cem Concr Compos* 2009;31:195–203.
- [14] Nili M, Ehsani A. Investigating the effect of the cement paste and transition zone on strength development of concrete containing nanosilica and silica fume. *Mater Des* 2015;75:174–83.
- [15] Antonopoulou Sofia. Self-healing in ECC materials with high content of different micro-fibres and micro-particles. *Delft University of Technology*; 2009.
- [16] Brinker CJ, Frye GC, Hurd AJ, Ashley CS. Fundamentals of sol-gel dip coating. *Thin Solid Films* 1991;201:97–108.
- [17] Milea CA, Bogatu C, Duță A. The influence of parameters in silica sol-gel process. *Eng Sci* 2011;4(53):59–66.
- [18] Flores-Vivián Ismael, Sobolev Konstantin. The effect of nano-SiO₂ on cement hydration. *Nanotechnology in construction*. Springer; 2015. 167–172.
- [19] Buckley AM, Greenblatt M. Sol-gel preparation of silica gels. *J Chem Educ* 1994;71(7):599–602.
- [20] Danks AE, Hallb SR, Schnepf Z. The evolution of 'sol-gel' chemistry as a technique for material synthesis. *R Soc Chem: Mater Horizons* 2016;3:91–112.
- [21] Coppola B, Di Maio L, Scarfato P, Incarnato L. Use of polypropylene fibers coated with nano-silica particles into a cementitious mortar. In: Proceeding of the GT70 international conference 15–17 October 2015. Italy.
- [22] Yang Zhiqian, Liu Jianzhong, Liu Jiaoping, Li Chanfeng, Zhou Huaxin. Silica modified synthetic fiber for interface property in FRCC. In: Proceeding of BEFIB2012-fibre reinforced concrete; 2012.
- [23] ASTM D570-98. Standard Test Method for Water Absorption of Plastics. ASTM International, West Conshohocken, PA, United States; 2010.